

# Single pulse nm-size grating formation in polymers using laser ablation with an irradiation wavelength of 355 nm

T. Lippert,<sup>a)</sup> T. Gerber, and A. Wokaun  
Paul Scherrer Institute, 5232 Villigen PSI, Switzerland

D. J. Funk  
Los Alamos National Laboratory, MS C920, Los Alamos, New Mexico 87545

H. Fukumura<sup>b)</sup> and M. Goto  
Advanced Science Research Center, Japan Atomic Energy Research Institute, Neyagawa, Osaka 572, Japan

(Received 16 April 1999; accepted for publication 18 June 1999)

Laser ablation at 355 nm of a specially designed polymer was used as a true single step dry-etching process to create a two-beam interference grating. Gratings with groove spacings of 180 and 1090 nm were created with single laser pulses. Moreover, by varying the laser fluence and/or the angle between the two beams, variable modulation frequencies (depth/spacing) could be obtained. Additional pulses deteriorated the grating quality, demonstrating the importance of the single pulse approach. © 1999 American Institute of Physics. [S0003-6951(99)00333-2]

Gratings, especially diffraction gratings, are fabricated using two different processes. Mechanically ruled gratings are fabricated with diamond tools, whereas interference (sometimes called holographic) gratings are fabricated with light. Interference gratings have the advantage that there exist no errors in ruling compared to mechanically fabricated grooves. In addition, interference gratings are entirely free of small periodic or random groove placement errors, found on even the best mechanically ruled gratings.<sup>1</sup> This gives significant advantages for spectroscopic systems in which light is performance limiting (e.g., Raman spectroscopy of solids).

Gratings having micron to submicron periodicity have other important applications in optoelectronic devices (e.g., Bragg type filters)<sup>2</sup> and for alignment of liquid crystals.<sup>3</sup> The standard technique for the fabrication of these gratings is the irradiation of a photoresist followed by various development and dry etching processes.<sup>4</sup> These are relatively complicated, time consuming technologies. Many different approaches for the direct writing of gratings in polymers and glasses have been developed. For example, using polarized UV laser beams and fluences *below* the threshold of polymer ablation, laser induced periodic surface structures (LIPSSs) are formed.<sup>5,6</sup> Gratings with spacings in the submicron range can be produced in this way. The process has some difficulty in reproducing gratings with exactly the same spacing<sup>7</sup> and it is still a relatively time consuming process, needing several hundreds of laser pulses. Laser ablation, on the other hand, offers an alternative, simple technique for grating generation. Grating like structures can be produced under ablation conditions (laser fluences above the ablation threshold) from stretched polymer films.<sup>8-10</sup> A completely different approach uses a photocurable monomer and a contact mask (using the volume contraction of the polymer and diffusion of the monomer into the polymerization area).<sup>11</sup> Faster techniques

for highly reproducible gratings use phase masks,<sup>12,13</sup> Talbot interferometers,<sup>14,15</sup> transmission gratings with imaging optics,<sup>16</sup> and Michelson interferometers.<sup>17</sup> All of these techniques use laser fluences above a certain material dependent threshold. The resulting gratings range in size from micron to sub 100 nm size spacing, and are highly reproducible. Single pulse grating formation has been reported only recently.<sup>2</sup>

We have studied single and multiple ( $\leq 10$  pulses) pulse grating formation in a photodecomposable polymer at 355 nm using a Michelson setup (shown in Fig. 1). The polymer was chosen because of its high sensitivity,<sup>18,19</sup> the possibility of a photochemical ablation mechanism,<sup>20</sup> and the absence of solid ablation products<sup>21</sup> which could contaminate the surface lowering the grating quality, or necessitate additional cleaning steps.

The synthesis of the polymer (structure shown as insert in Fig. 1) has been described previously.<sup>22</sup> Thin films of the polymer ( $\approx 1-2 \mu\text{m}$ ) were prepared by spin coating, also described in detail elsewhere.<sup>23</sup> The roughness of the spin-coated films was measured using atomic force microscopy (AFM). The mean roughness was between 1.5 and 2.0 nm over a  $10 \mu\text{m}$  scan length. The ablation experiments used a frequency tripled Nd:YAG laser (3 ns pulse length and 1 Hz repetition rate) in a Michelson setup (shown in Fig. 1). The linear absorption coefficient of the polymer at 355 nm is

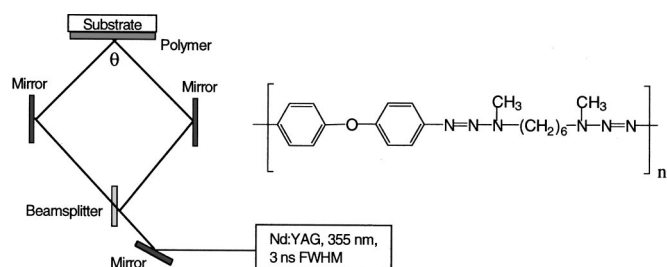


FIG. 1. Experimental setup with inserts of the chemical structure of the polymer.

<sup>a)</sup>Electronic mail: lippert@psi.ch

<sup>b)</sup>Permanent address: Department of Chemistry, Tohoku University, Sendai 980-8578, Japan.

$\approx 1.15 \times 10^5 \text{ cm}^{-1}$ . The spacing of the grating  $s$  can be varied according to the equation

$$2 = \frac{1}{2} \lambda \sin^{-1}(\theta/2) \quad (1)$$

by changing the intersection angle  $\theta$  ( $\lambda$  is the laser wavelength, here fixed at 355 nm). The grating formation (depth and spacing) was determined by AFM. We generated two different spacings  $d$ , of  $\approx 1.09 \mu\text{m}$  and  $\approx 180 \text{ nm}$ , respectively, at two different laser fluences and with single and multiple laser pulses. The grating spacing of 180 nm was chosen because it is close to the theoretical limit of  $\lambda/2$ .

Well-defined interference gratings with spacings corresponding to the expected values were found for single pulse experiments. We believe that the quality of the gratings is at least as good as the best previously reported gratings formed in polymers by direct writing methods. The gratings formed here are much deeper than the gratings described in Refs. 12–17. The only other study that we are aware of using single pulses tried polyimide as a substrate. Gratings with a spacing of  $1 \mu\text{m}$  and a depth of about 80 nm could be achieved. However, scanning electron microscope results suggested that some ablation products (debris) were contaminating the grating surface.<sup>2</sup> The specially designed polymer used in our experiment results in a debris-free ablation, promising a one step process; i.e., no postprocessing is necessary. This arises from the fact that the polymer produces gaseous products, which do not condensate on the surface. In other studies, multiple pulses (four to several hundreds) have been used, but the grating depths were still quite limited (20–100 nm).<sup>11–16</sup> In addition, multipulse techniques seem to have problems with the quality of the gratings. Sometimes, substructures on top of the remaining ridges are detected,<sup>13,14</sup> or the grooves are wider than the remaining ridges.<sup>15</sup> We also encountered problems with grating quality when using multiple pulses, which will be discussed later.

Using laser ablation as a fabrication technique provides the unique advantage that the grating depth can be varied continuously by adjusting the laser power. Realistic depths, for specially designed polymers and not too shallow angles  $\theta$ , are in the range of several hundred nm for a single pulse. Moreover, reference data for etch rate versus laser fluence allows the depths of the grooves to be predetermined. In addition, the spacing of the grating is also easily accessed by varying the angle  $\theta$ . Thus, spacings of  $\approx \lambda/2$  to  $\approx 10 \mu\text{m}$  for our setup are readily achievable.

While ruled gratings are separated into different families according to their blaze angle, interference gratings are categorized by using the modulation frequency  $\alpha$  defined as

$$\alpha = d/s, \quad (2)$$

where  $d$  is depth and  $s$  is spacing of the grating.<sup>1</sup>

In general, five different ranges are used to categorize an interference grating:

- (i)  $\alpha \leq 0.05$ , with a peak reflectivity wavelength at  $3.4d = 3.4\alpha s$  (a blazed grating with an equivalent peak wavelength will require a groove depth 1.7 times greater);
- (ii)  $0.05 \leq \alpha < 0.15$ , with a flat efficiency for the first order of  $\lambda/s$  from 0.35 to 1.4;

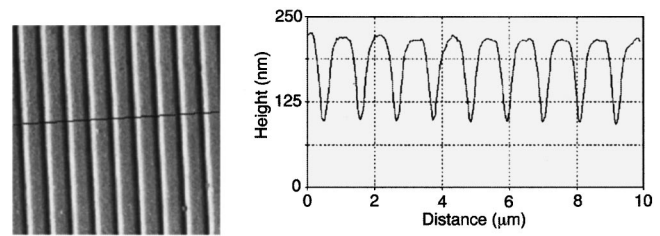


FIG. 2. AFM image of grating of 1090 nm spacing: one pulse with  $80 \text{ mJ cm}^{-2}$  with the X–Z plot as inset.

- (iii)  $0.15 \leq \alpha < 0.25$ , with a reasonable efficiency for  $\lambda/s > 0.45$ ;
- (iv)  $0.25 \leq \alpha < 0.40$ , with the maximum efficiency of all interference gratings for  $0.65 < \lambda/s$ ;
- (v)  $\alpha > 0.4$ , with little applications, except sometimes for grazing incidence applications.

Two different laser fluences ( $80$  and  $240 \text{ mJ cm}^{-2}$ ) and therefore two different depths were achieved when creating the gratings. Figure 2 shows AFM data for the experiment with a single pulse and a fluence of  $80 \text{ mJ cm}^{-2}$ . The insert in Fig. 2 shows the X–Z plot of the data. As seen in Figs. 1 and 2, the grating is of high quality, with no debris contaminating the surface, nor is there any evidence of substructures. The grooves and ridges are equidistant and the tops of the ridges are relatively flat and not rounded. The depth of the grating is  $\approx 135 \text{ nm}$ , corresponding to a modulation frequency  $\alpha$  of 0.12.

Higher laser fluences yielded deeper gratings as expected, but we observed slight differences in the width of the grooves. Specifically, at  $80 \text{ mJ cm}^{-2}$ ,  $0.7 \mu\text{m}$  wide grooves are found, while  $0.85 \mu\text{m}$  wide grooves are observed at  $240 \text{ mJ cm}^{-2}$ . This has been previously reported and attributed to the ablation threshold,<sup>13,14</sup> which will cause wider areas to be ablated at the higher fluences. Assuming a Gaussian laser intensity profile, the diameter of the beam with intensities above a constant threshold increases with increasing energy. For the  $240 \text{ mJ cm}^{-2}$  irradiation a grating depth of around  $450 \text{ nm}$  results, corresponding to a modulation frequency of 0.41. This demonstrates how easily modulation frequencies are accessed with the laser ablation approach and through the use of specially designed polymers.

The 180 nm spaced gratings reveal much shallower depths at the same given laser fluence than the micron size gratings. For example, applying  $80 \text{ mJ cm}^{-2}$  results in a groove depth of 30 nm, while for the micron-sized gratings a depth of 125 nm was found. The nm grating experiments are conducted close to the theoretical spacing limit, and therefore require an angle  $\theta$  close to  $180^\circ$ . We modeled the interference pattern of two overlapping plane waves at the angle  $\theta$ , corresponding to the  $1 \mu\text{m}$  and 180 nm grating. Adding up the fields and attenuating the fields for the penetration into the material, using the linear absorption coefficient, revealed differences in the etch depth between the two gratings. The experimental results could be reproduced very well with an additional scaling factor for the etch depth. This shows that the difference in the grating depths for the 180 nm and  $1 \mu\text{m}$  grating at the same laser fluence is caused by the longer path within the material, and hence less deep penetration of the

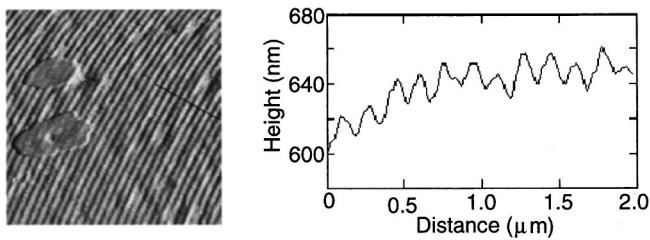


FIG. 3. AFM image of grating of 180 nm spacing: one pulse with  $155 \text{ mJ cm}^{-2}$  with the X-Z plot as inset.

interference field into the material for the shallow angles.

Nevertheless, gratings with nm-size spacing were fabricated. Figure 3 shows the AFM data and X-Y plot for a single pulse grating with an irradiation fluence of  $155 \text{ mJ cm}^{-2}$ . The unstructured patches in Fig. 3 are most probably due to impurities or decomposed polymer that exhibit no absorption at the irradiation wavelength. The structure shows quite a lot of irregularities. This is due to the mentioned mechanism for irradiation at very shallow angles. The surface roughness (2 nm) and surface contaminations will cause substantial shading at grazing incidence irradiation.

The grating depths of 30 and 60 nm for irradiation with 80 and  $155 \text{ mJ cm}^{-2}$ , correspond to modulation frequencies of 0.17 and 0.33, respectively.

In an attempt to improve the modulation frequency, by increasing the grating depths, experiments with multiple pulses (2–10) have been performed. After multiple pulses a pronounced deterioration of the grating was detected, as shown in Fig. 4. For the  $1 \mu\text{m}$  grating the depth increased slightly with the second pulse, but the structure showed recognizable deterioration of the grating quality. Upon further irradiation the depth as well as the quality of the gratings were reduced. This effect is even more pronounced for the 180 nm gratings.

The deterioration of the grating (shown in Fig. 4) with successive pulses cannot be attributed to thermal effects, since in an experiment using a mask and projection technique ( $1 \mu\text{m}$  slit pattern and multiple pulses with  $200 \text{ mJ cm}^{-2}$ ) sharp contours remained. Additionally, the thermal diffusion length for the laser pulse corresponds only to 30–40 nm for commercial polymers such as poly(ethylene-terephthalate).

At the present stage of our research program we can only offer tentative explanations for these observations. Laser instabilities, such as thermal lensing, can definitely change the beam path between successive pulses, which will laterally shift the grating from pulse to pulse. We don't believe, however, that a shadowing effect of the already existing grating

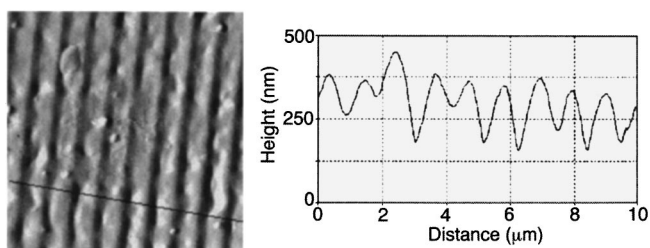


FIG. 4. AFM image of grating of 1090 nm spacing: five pulses with  $80 \text{ mJ cm}^{-2}$  with the X-Z plot as inset.

on successive pulses is responsible, especially in the case of the micron size grating, where  $\theta$  is only  $18^\circ$ . Diffracted light from the grating formed in the first pulse may not reach the ablation threshold, as the diffraction efficiency for orders  $n > 1$  amounts to less than 5%. Another possible reason could be the fact that the film thickness is only  $1\text{--}2 \mu\text{m}$ , and the absorption coefficient is  $115\,000 \text{ cm}^{-1}$ . Therefore, some light will penetrate the film and be partially reflected from the substrate. Light below the threshold of ablation will decompose the chromophores and thereby bleach the material, but not cause ablation. Therefore, polymer areas with different absorption at the laser wavelength or partially crosslinked polymers, with different properties, are formed. These material properties will also influence the possible application of the gratings. UV light causes decomposition of the polymer and will therefore damage the grating and reduce its durability. Therefore an application as reflective grating would be desirable, where metallization would act as UV protection to increase the durability.

Formation of two beam interference gratings in a special designed polymer using a direct writing method (laser ablation) have been demonstrated. Well-defined gratings with variable spacings and depths (and therefore modulation) can be achieved with single pulses. No further cleaning steps are necessary, because the products of ablation are gaseous. Additional pulses deteriorate the gratings, demonstrating the importance of the single pulse approach.

<sup>1</sup> *Diffraction Grating Handbook*, edited by C. Palmer and E. Loewen (Richardson Grating Laboratory, Rochester, 1996).

<sup>2</sup> K. O. Hill, Y. Fujii, D. C. Johnson, and B. S. Kawasaki, *Appl. Phys. Lett.* **32**, 647 (1978).

<sup>3</sup> C. J. Newsome, M. O'Neill, R. J. Farley, and G. P. Bryan-Brown, *Appl. Phys. Lett.* **72**, 2078 (1998).

<sup>4</sup> J. Söchtig, H. Schütz, R. Widmer, R. Lehmann, and R. Grosse, *Proc. SPIE* **2213**, 98 (1994).

<sup>5</sup> S. Lazare, M. Bolle, A. Cros, and L. Bellard, *Nucl. Instrum. Methods Phys. Res. B* **105**, 159 (1995).

<sup>6</sup> S. Lazare and D. Drillhole, *J. Photochem. Photobiol., A* **106**, 15 (1997).

<sup>7</sup> M. Sendova and H. Hiraoka, *Jpn. J. Appl. Phys., Part 1* **32**, 6182 (1993).

<sup>8</sup> H. Niino, Y. Kawabata, and A. Yabe, *Jpn. J. Appl. Phys., Part 2* **28**, L2225 (1989).

<sup>9</sup> T. Lippert, F. Zimmermann, and A. Wokaun, *Appl. Spectrosc.* **47**, 1931 (1993).

<sup>10</sup> D. Knittel, W. Kesting, and E. Schollmeyer, *Polym. Int.* **43**, 231 (1997).

<sup>11</sup> T. Okamoto, R. Ohmori, S. Hayakawa, I. Seo, and H. Sato, *Opt. Rev.* **4**, 516 (1997).

<sup>12</sup> P. E. Dyer, R. J. Farley, and R. Giedl, *Opt. Commun.* **129**, 98 (1996).

<sup>13</sup> P. E. Dyer, R. J. Farley, R. Giedl, and D. M. Karnakis, *Appl. Surf. Sci.* **96–98**, 537 (1996).

<sup>14</sup> H. M. Phillips, D. L. Callahan, R. Sauerbrey, G. Szabò, and Z. Bor, *Appl. Phys. Lett.* **58**, 2761 (1991).

<sup>15</sup> H. M. Phillips, D. L. Callahan, R. Sauerbrey, G. Szabò, and Z. Bor, *Appl. Phys. A: Solids Surf.* **54**, 158 (1992).

<sup>16</sup> K. Chen, J. Ihlemann, P. Simon, I. Baumann, and W. Sohler, *Appl. Phys. A: Mater. Sci. Process.* **65**, 517 (1997).

<sup>17</sup> K. J. Ilcisin and R. Fedosejevs, *Appl. Opt.* **26**, 396 (1987).

<sup>18</sup> T. Lippert, L. S. Bennett, T. Nakamura, H. Niino, A. Ouchi, and A. Yabe, *Appl. Phys. A: Mater. Sci. Process.* **63**, 257 (1996).

<sup>19</sup> T. Lippert, J. Stebani, J. Ihlemann, O. Nuyken, and A. Wokaun, *J. Phys. Chem.* **97**, 12296 (1993).

<sup>20</sup> H. Furutani, H. Fukumura, H. Masuhara, T. Lippert, and A. Yabe, *J. Phys. Chem. A* **101**, 5742 (1997).

<sup>21</sup> L. S. Bennett, T. Lippert, H. Furutani, H. Fukumura, and H. Masuhara, *Appl. Phys. A: Mater. Sci. Process.* **63**, 327 (1996).

<sup>22</sup> J. Stebani, O. Nuyken, T. Lippert, and A. Wokaun, *Rapid Commun. Mass Spectrom.* **14**, 365 (1993).

<sup>23</sup> D. M. Karnakis, T. Lippert, N. Ichinose, S. Kawanishi, and H. Fukumura, *Appl. Surf. Sci.* **127–129**, 781 (1998).